

Solvent assisted post-polymerization of PET

Y. Ma, U.S. Agarwal*

Faculty of Chemical Engineering, Polymer Technology Group/Dutch Polymer Institute, Eindhoven University of Technology, 5600 MB Eindhoven, The Netherlands

Received 24 February 2005; received in revised form 28 April 2005; accepted 1 May 2005
Available online 23 May 2005

Abstract

We have examined the influence of the solvent mixture diphenyl ether–biphenyl (DPE–BP) on the post-polymerization of poly(ethylene terephthalate) (PET) of intrinsic viscosity (IV = 0.42 dL/g) in the swollen state and in solution, by following the IV increase and the end-group depletion. During the swollen state polymerization (SwSP) of thin disks (180 μm) at 195 °C, the initially rapid step growth polymerization slows dramatically beyond IV = 1.2 dL/g in 5 h, and is unable to proceed beyond 1.4 dL/g. This appears to be related to the temporarily restricted mobility of the end groups due to the observed solvent induced crystallization, because sufficient reactive end groups can be directly detected, and further post-polymerization in melt state is possible. When limitations due to crystallization are eliminated by carrying out post-polymerization in solution at 250 °C, it proceeds to IV = 1.8 dL/g in a single step. Since solution polymerization eliminates the requirement of handling fine PET particles, it offers an attractive route to high molecular weight PET, particularly when the solution can be directly used for further processing, e.g. into fibers.

© 2005 Published by Elsevier Ltd.

Keywords: Poly(ethylene terephthalate); Swollen-state polymerization; Solution polymerization

1. Introduction

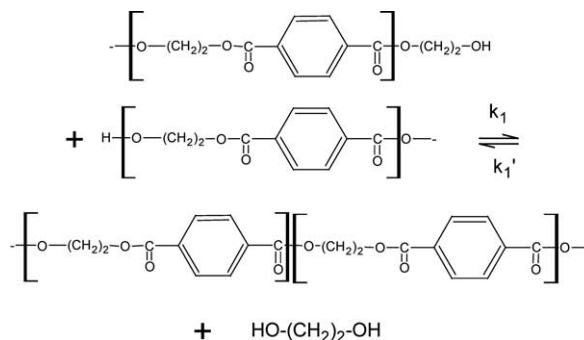
Poly(ethylene terephthalate) (PET) is widely used as films, fibers and engineering materials. While melt polymerized PET with intrinsic viscosity (IV) of about 0.6 dL/g can be directly used for textile application, a post-polymerization step is required to enhance the molecular weight for applications such as soft drink bottles, tire cord filaments and industrial fibers. IV of up to 1.2 dL/g required for these applications is often achieved by industrial post-polymerization processes in solid PET particles of dimension exceeding 1 mm. Even higher molecular weights of PET are desired for potential applications for high modulus high strength fibers through solution spinning [1–3]. Solid-state polymerization to IV greater than 1.5 dL/g often requires reaction temperatures close to the PET melting point, as well as reduction of the effective PET diffusion

length to less than 1 mm through film formation or porosity generation [1,4–12]. The problems associated with fusion of these fine particles at these high temperatures demand special solids handling procedures.

1.1. Reactions during post-polymerization of PET

The following reactions are generally considered to take place [12–20] when the solid PET pellets are heated to $T = 200–250$ °C.

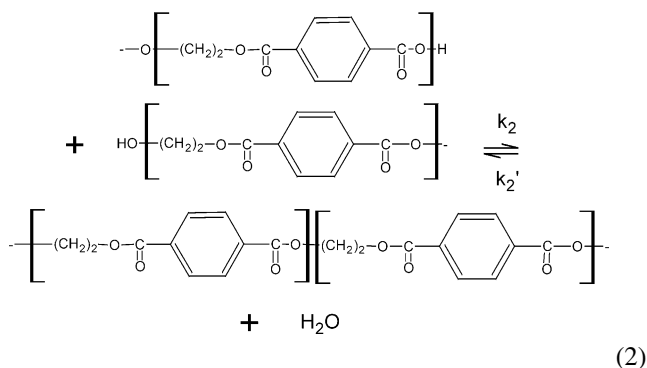
1.1.1. Transesterification/polycondensation



* Corresponding author. Tel.: +31 40 247 3079.

E-mail address: u.s.agarwal@tue.nl (U.S. Agarwal).

1.1.2. Esterification



Here, water and ethylene glycol (EG) are the by-products of the reversible reactions. The forward reactions are facilitated by the by-product removal either by vacuum or by flow of inert gases. The overall reaction rate is influenced by a combination of the intrinsic reaction rate [4,15,21–28], diffusion of the reactive end-groups [21,25,29–34] as limited by crystallization [12,16,35–37] or facilitated by interchange reactions [32], the diffusion of the by-products from the pellet interior to the pellet surface [15,23,26,27,34,38,39] and their removal by the inert gas stream [4,25–27,34]. In the absence of condensate diffusional limitations resulting in fast removal of water and EG, backward reactions are eliminated, and the reaction kinetics is described by the following expressions [16,25,26,33]:

$$\frac{d[\text{OH}]}{dt} = -2R_{\text{EG}} - R_{\text{H}_2\text{O}} \quad (3)$$

$$\frac{d[\text{COOH}]}{dt} = -R_{\text{H}_2\text{O}} \quad (4)$$

$$M_n = \frac{2}{[\text{OH}] + [\text{COOH}]} \quad (5)$$

where

$$R_{\text{EG}} = 2k_1[\text{OH}]^2 \quad (6)$$

and

$$R_{\text{H}_2\text{O}} = k_2[\text{COOH}][\text{OH}] \quad (7)$$

are the rates of production (or rates of removal) of EG and water, respectively. In Eq. (6), the additional factor of two is taken to account for the two pairs of reaction sites for a given pair of chain-ends [40], the rate constants being taken as those corresponding to the reactive groups.

1.2. Role of crystallization during SSP

The extent of crystallinity and the crystalline morphology are known to influence the rate of SSP [18,20,24]. For example, it is believed that the end-groups, and hence

the chemical reactions (1) and (2) during SSP, are restricted to the amorphous phase of PET. This enhances the effective end group concentration in the amorphous phase and hence in the reaction rate [41]. Several authors have followed the kinetics of SSP while monitoring the reduction in the OH and the COOH end-group concentrations with progress of SSP to moderate molecular weights [15,26,33,35,37]. The role of crystallization induced end-group concentration enhancement can be considered to be imbedded in their effective rate constants. An additional consideration that becomes increasingly important during SSP to high IV is the role of crystallization in limiting the accessibility of the end-groups to each other. Duh [28] accounted for this role of crystallization, but ignored the esterification reaction (Eq. (2)), and did not directly measure concentrations of the end-groups, and limited his analysis to IV less than 1.3 dL/g. However, he did not face a contradiction in fitting the kinetics, because he limited their analysis to molecular weights less than 52,000. We recently reported [12] that the rapid slowdown in SSP kinetics at IV greater than 1.3 dL/g could be represented by transesterification and the esterification reactions ((1) and (2)) only when accounting for the part of the acid and hydroxyl end groups ($[\text{COOH}]_i$ and $[\text{OH}]_i$) to be rendered temporarily inactive, resulting in the following rate expressions in place of Eqs. (6) and (7):

$$R_{\text{EG}} = 2k_1([\text{OH}] - [\text{OH}]_i)^2 \quad (8)$$

$$R_{\text{H}_2\text{O}} = k_2([\text{COOH}] - [\text{COOH}]_i)([\text{OH}] - [\text{OH}]_i) \quad (9)$$

A temporary inactivation of a part of the end groups through mobility restriction could arise either due to relatively short chain segments linking them to crystalline parts, or as a result of their having been incorporated in crystalline parts as defects. Though the concentration of such groups is small, they make up an increasing fraction of the total number of end-groups with progress of SSP.

1.3. Solvent assisted polymerization of PET

As discussed in Section 1.1, the polymerization rates in the solid state are often limited by the low diffusivity of water and EG out of the chips and by the low mobility of the reactive hydroxyl and carboxyl end groups of the polymer chains. A recent innovation for obtaining ultra high molecular-weight (UHMW) PET is the swollen state polymerization (SwSP) [42–45]. Here, the polymerization of PET chips is carried out by swelling in a suitable solvent that does not dissolve the chips. The rate of such SwSP is higher than SSP at the same temperature, and found to depend on the nature of solvent and the extent of swelling. More importantly, the highest achievable IV by SwSP is found to be dependent on several parameters, e.g. solvent used [42], particle size [43,44,46], initial IV [46], degree of swelling [42,44,47], catalyst concentration [47,48] and

reaction temperature [43,46,47]. For example, Tate and Watanabe [44] found that while PET fibres could be post-polymerized in swollen state in hydrogenated terphenyl at 236 °C for 15 h to IV = 3.1 dL/g, PET granules (3 mm) could not be polymerised to IV greater than 2.1 dL/g. Ha et al. [46] found that porous and fibrous PET with starting IV = 0.62 dL/g could be similarly post-polymerized in swollen state in hydrogenated terphenyl at 230 °C for 6 h to IV = 1.82 dL/g, but not higher. Wang et al. [47] found that PET of starting IV = 0.62 dL/g could not be post-polymerized in swollen state in diphenyl ether–biphenyl (DPE–BP) mixture at 200 °C to IV values exceeding 1 dL/g. The enhancement in polymerization rate by swelling with a solvent may be due to the increased surface area (high mass transfer rates of condensates), enhanced diffusivity of condensate molecules (enabling their easy removal), increased mobility of reactive chain ends (accelerating their collisions), and intrinsic catalytic effects of solvent presence/participation in reaction. Since we found the SwSP rates to be larger than SSP rates even in very thin PET disks where the condensate diffusion (mass transfer) limitations were eliminated, we attributed the increased post-polymerization rates of thin PET during SwSP to the increased mobility of the chain ends due to the presence of the solvent [48]. However, the same solvent that assists chain mobility at low IV, can increase PET crystallization by solvent induced crystallization [42,44]. In line with the crystallization induced limitation during SSP, the high crystallization during SwSP perhaps brings in stronger limitations in the highest IV achievable during SwSP. If so, it is interesting to examine if the post-polymerization can be carried out to higher IV in solutions, thus eliminating the limitation imposed by solvent induced crystallization. Since the toxicity of the thermal fluids (such as DPE, BP) is small, post-polymerization in these solvents can be especially interesting if the high molecular weight PET polymerized in these solvents can be directly spun into high modulus high strength fibers. Tate et al. [49] reported extrusion of PET (IV = 2 dL/g) melt plasticized with 1-methyl naphthalene (20 wt%) at 270 °C, followed by solvent evaporation and drawing to a draw ratio of about six, resulting in tensile modulus and strength of 30 and 2 GPa, respectively. Rogers [50] reported solution spinning of a 30% solution of PET of IV = 1.71 dL/g into filaments that could be drawn into fiber of modulus 90 g/dtex.

In this paper, we follow the progress of SwSP by monitoring not only the IV, but also the acid and hydroxyl end-groups concentrations using our recently developed NMR based technique [51]. The results are analyzed in terms of the kinetics of the two simultaneous reactions producing EG and water (Eqs. (1) and (2)), and the limiting IV obtained is explained in terms of the crystallization induced temporary inactivation of part of the end groups. Solution polymerization of PET in the same solvents is then examined to eliminate the role of crystallization.

2. Experimental

2.1. Materials

PET chips (IV = 0.42 dL/g) were obtained from Wilton Research Center (ICI, UK). Chloroform (CHCl₃, 99.9%), deuterated chloroform (CDCl₃, 99.9 atom D%), hexafluoroisopropanol (HFIP, 99%), α,α,α -trifluorotoluene (TFT, 99%), 4-pyrrolidinopyridine (98%), trifluoroacetic acid (TFA, 99%) and bishydroxyethyl terephthalate (BHET) were obtained from Aldrich. Dicyclohexyl carbodiimide (DCC, 99%), diphenyl ether (DPE, 98%), biphenyl (BP, 99%), tetrachloroethane (TCE, 97%) were obtained from Merck. All chemicals were used as received. DPE and BP were mixed in the weight ratio (73.5:26.5) to obtain a eutectic mixture, and dried over molecular sieves (4 Å) over 3 days to obtain the mixed solvent DPE–BP.

2.2. NMR analysis

400 MHz Varion Mercury V × 400 was used to carry out the ¹⁹F NMR measurements, using CDCl₃ mixture with HFIP or TFA as the solvents.

2.3. Intrinsic viscosity (IV) of PET

The relative viscosity (η_{rel}) of solution of PET in phenol–TCE mixture (1:1, by weight) at concentration ($c = 0.5$ g/dL) was determined using Ubbelohde viscometer at 30 °C. IV was estimated from this single point measurement of η_{rel} and using the following approximation for linear flexible chains [52]:

$$IV = \left(\frac{1}{c}\right) [2(\eta_{rel} - 1) - 2 \ln(\eta_{rel})]^{1/2} \quad (10)$$

which can be related to M_n using the Mark–Houwink relationship [12,53–55]:

$$IV = KM_n^a \quad (11)$$

2.4. DSC

The melting characteristics of the samples were examined using Perkin–Elmer differential scanning calorimetry system DSC-7. The heat of melting and heat of crystallization were determined from the corresponding peak area during heating scan at 20 °C/min.

2.5. WAXD

The WAXD measurements were carried out with a Rigaku D/Max-B diffractometer, using Cu K α radiation at 40 kV and 30 mA. The samples were measured with a step size of 0.02 (degree 2 θ) and a dwell time of 2 (s).

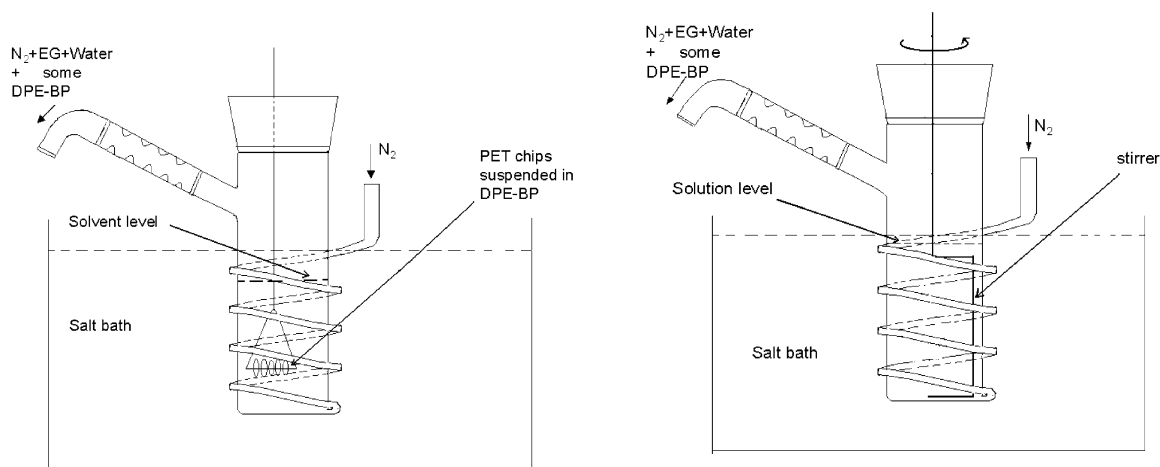


Fig. 1. Schematic of apparatus used for post-polymerization of PET in swollen state (left) and in solution (right).

2.6. Swollen state polymerization (SwSP)

As shown in Fig. 1, the reaction apparatus is a vertical glass tube (25 cm long, id=27 mm), fitted with a helical coil for bubbling nitrogen, and a condenser for refluxing the solvent. The reactor was immersed in a salt bath maintained at 195 °C, and the solvent DPE–BP (15 mL) was added. Nitrogen gas flowing at the rate of 2 L/min (room temperature and pressure) was dried by passing through an anhydrous CaSO₄ column (W.H. Hammod Drierite, Xenia, OH, USA), preheated by passing through a glass coil immersed in the same bath, and introduced at the bottom of the reactor. PET chips (average weight 0.045 g) were pressed for 1 min into thin disks (diameter ~1.5 cm, thickness ~180 μm) between two stainless steel plates heated to 160 °C. These PET disks (0.8 g) were dried overnight under vacuum at 150 °C, and suspended (by hanging independently from metallic wires) into the solvent mixture in the reactor. The PET disks were taken out at the desired reaction time, and dried under vacuum.

2.7. Solution polymerization (SolP)

Similar to SwSP, the reaction apparatus is a vertical glass tube (25 cm long, id=27 mm), fitted with a helical coil and a condenser. In addition, it is fitted with a custom made stirrer that closely scrapes the wall while being driven by an electric motor (Fig. 1). The reactor was immersed in a salt bath maintained at 250 °C, and the solvent mixture DPE–BP (25 mL) was added. Nitrogen gas flowing at the rate of 2 L/min (room temperature and pressure) was dried by passing through an anhydrous CaSO₄ column (W.H. Hammod Drierite, Xenia, OH, USA), preheated by passing through a glass coil immersed in the same bath, and introduced at the bottom of the reactor. PET chips (10.8 g), pre-dried overnight under vacuum at 150 °C, were added to the reactor while stirring at 200 rpm, when the PET chips dissolved within 5 min. Trials with a few condenser

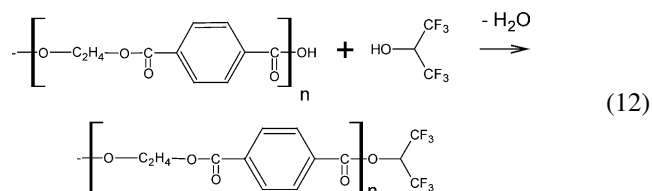
conditions (length, insulation/convection cooling) lead to one that allowed reflux of most of the solvent while allowing a small amount (~5%, over the 30 h reaction) of the solvent to escape the reflux condenser, the escaping solvent eventually being trapped in a long chilled water cooled condenser leading to a collection flask. Considering the small amounts and the lower boiling nature of the reaction condensates (EG and water), it is expected that these were efficiently stripped from the reaction mixture, into the collection flask. At the desired time, the concentrated PET solution sample was withdrawn with the stirrer after detaching the motor. The solution solidified immediately, and was dried under vacuum at 150 °C for 6 h.

2.8. Solid state polymerization in vacuum (SSP-vacuum)

Thin PET disks were placed in a glass made 150 mL round bottomed flask connected to a vacuum pump maintaining 10 mTorr pressure. The flask was immersed till its neck into a preheated, temperature controlled salt bath. The disks were first dried at 165 °C for 6 h. The flask was then transferred to an identical bath, but maintained at 252 °C (resulting in 250 °C inside the flask), and the flask was withdrawn after the desired time of reaction.

2.9. Determination of acid end-groups in PET

The fluoroderivatization of the acid end-groups was carried out by DCC mediated esterification with HFIP [51]:

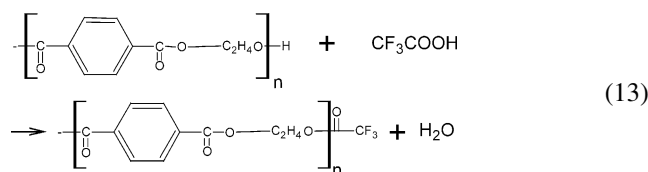


One chip of PET (0.045 g) was dissolved in a mixture of HFIP (0.2 g) and CDCl₃ (1.00 g) at room temperature.

Firstly, part (0.1 g) of a solution of 4-pyrrolidinopyridine (0.001 g) in CDCl_3 (1 g) was added and subsequently, part (0.2 g) of a solution of DCC (0.0075 g) in CDCl_3 (1.5 g) was added. Finally, part (0.1 g) of a solution of TFT (0.01 g) in CDCl_3 (2 g) was added to the above reaction mixture to give the sample for ^{19}F NMR analysis. Integration of the $\delta -73.41$ [d, 6F] peak for the fluoroester relative to the $\delta -62.9$ [s, 3F] peak of TFT allowed quantification of the acid end-groups.

2.10. Determination of hydroxyl end-groups in PET

The hydroxyl end-groups were fluoroderivatized by esterification with TFA [51,56]:



One chip of PET (0.045 g) was dissolved in a mixture of TFA (0.2 g) and CDCl_3 (1.0 g). Part (0.1 g) of a solution of TFT (0.01 g) in CDCl_3 (2 g) was added to the above reaction mixture. ^{19}F NMR analysis was carried out after standing for 72 h. Integration of the $\delta -75.2$ [s, 3F] peak for the fluoroester relative to the $\delta -62.9$ [s, 3F] peak of TFT allowed quantification of the acid end-groups.

3. Results and discussion

3.1. SwSP kinetics and crystallization induced chain-end immobility

Swelling of the pressed PET chip (0.045 g) to their equilibrium swollen weight (0.08 g) took place in less than

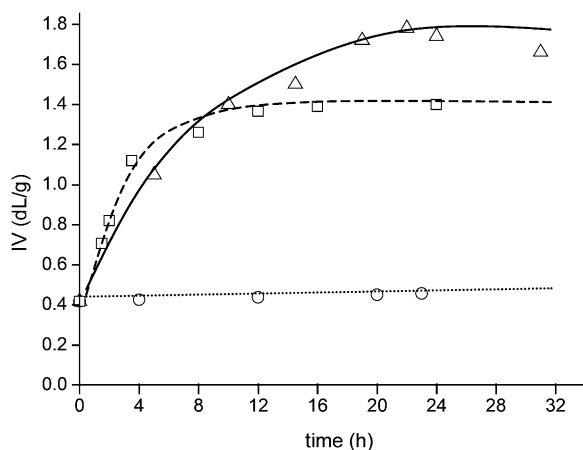


Fig. 2. Increase in IV with time of (a) SwSP (squares, - - -) in PET disks (180 μm thick) at 195 $^{\circ}\text{C}$ in DPE-BP, (b) SolP (triangles, —) at 30 wt% in DPE-BP at 250 $^{\circ}\text{C}$, (c) SSP (circles, dotted line) in PET disks (180 μm thick) at 195 $^{\circ}\text{C}$ under nitrogen. The lines are smoothly drawn to guide the eyes.

1 min after dipping in the hot DPE-BP (195 $^{\circ}\text{C}$), indicating a PET concentration of 56 wt% in the swollen chip. The IV vs. time data for the originally 180 μm thick pressed disks are shown in Fig. 2. Initially, the IV increases quickly from 0.42 to 1.2 dL/g in 5 h, and then nearly flattens out at a maximum IV of 1.4 dL/g at 12 h. Also shown in the figure are the kinetics data for SSP under the same conditions, but without the solvent. We notice that the SwSP proceeds much faster than SSP at the same temperature.

In case of thick PET (half thickness, $L > \sqrt{D/(kC)}$, where D and C are the condensate diffusivity and concentration, and k is the corresponding rate constant [23]), the SwSP can be limited by the outward diffusion of the condensates EG and water through the polymer. Calculation with $D_{\text{EG}} = 3.1 \times 10^{-6} \text{ cm}^2/\text{s}$ in PET alone [33] (higher in swollen PET), $k = 0.02 \text{ kg/meq h}$ (this paper), and $C = 163 \text{ meq/kg}$ (this paper) suggests that such diffusional limitations are negligible at the swollen chip thickness of less than 350 μm employed in SwSP. Hence, the observed rate of our SwSP reaction must be limited by the intrinsic reaction kinetics, and we will like to represent our SwSP kinetics data in terms of the reactions (1) and (2). Fig. 3 shows our measurements of the depletion of end groups with progress of the SwSP, as determined by fluoroderivatization of the acid and the hydroxyl end groups, followed by F NMR [51]. We first tried to represent the kinetics data ($[\text{OH}](t)$ and $[\text{COOH}](t)$) of SwSP with the kinetics expressions Eqs. (3)–(7). However, the flattening of $[\text{OH}](t)$ and $[\text{COOH}](t)$ curves at ~ 12 h even when substantial $[\text{OH}]$ and $[\text{COOH}]$ end-groups are present, could not be explained in terms of these second order rate expressions. As in our earlier work on SSP [12], such a phenomenon can be related to inability of a part of end-groups to participate in the condensation reactions (Eqs. (1) and (2)), due to crystallization induced mobility restrictions. Though the concentration of such groups is small, they make up an increasing fraction of the total number of end-groups with progress of the SwSP. Inability of a part of the end-groups to participate in the polycondensation reactions can be either due to chemical degradation leading to unreactive chain ends (such as vinyl end-groups), or due to the reactive ends being unable to approach each other. Such limited extent of mobility of some chain-ends could be a result of their being restricted by relatively short chain segments linking them to crystalline parts, or a result of their having been incorporated in crystalline parts as defects. We note from Fig. 3 that the OH and the COOH end-groups are still detectable (by fluoroderivatization and ^{19}F NMR), at substantial concentrations of about 26 and 11 meq/kg, respectively, at the end of our SwSP. We further verified this by the following experiment: the PET sample of IV = 1.4 dL/g (obtained by SwSP, $t = 15$ h as in Fig. 2), was dried at 150 $^{\circ}\text{C}$ under vacuum for 6 h, heated to melt on aluminium foil at 270 $^{\circ}\text{C}$ under vacuum for 4 h. The measured IV = 2.4 dL/g of that sample suggests a re-initiation of the polymerization in the molten. We conclude that the melting after SwSP results in

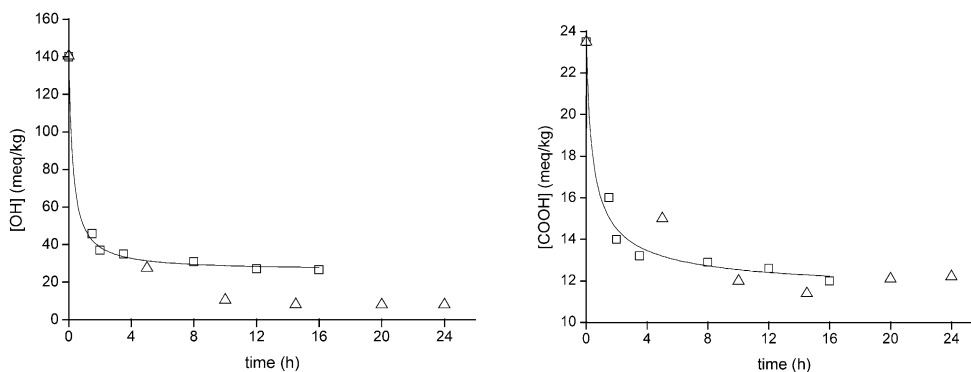


Fig. 3. Depletion of the (a) hydroxyl and (b) acid end-groups with post-polymerization during SwSP at 195 °C (squares) and SolP at 250 °C (triangles). The lines represent the fits to SwSP data while accounting for the inactive end-groups.

release of the crystalline restraints on the mobility of the temporarily inactivated acid and hydroxyl end-groups, allowing post-polymerization to start again.

This suggests that a kinetic analysis of SwSP should take into account this apparent inactivity of a fraction of the OH and COOH end-groups. The $[OH](t)$ and $[COOH](t)$ data for SwSP are now fitted (using the CONSTANT_RELATIVE_VARIANCE model of the gPROMS software, PSE Enterprises, UK) with the kinetics expressions Eqs. (3)–(5), (8) and (9) to estimate the rate constants: $k_1 = 0.008$ kg/meq h, $k_2 = 0.0203$ kg/meq h and the inactive end-group concentrations $[OH]_i = 26.4$ meq/kg and $[COOH]_i = 10.9$ meq/kg. The corresponding calculated $[OH](t)$, $[COOH](t)$ profiles are shown as curves in Fig. 3, and we conclude a satisfactory match with the experimental measurements obtained by us during SwSP. The lower value of the highest IV ($= 1.4$ dL/g) achievable by SwSP as compared to SSP (highest IV ~ 2.8 dL/g, Ref. [12]), and the much higher $[OH]_i$ meq/kg and $[COOH]_i$ meq/kg values as compared to SSP at 250 °C ($[OH]_i = 3.1$ meq/kg and $[COOH]_i = 2.8$ meq/kg) hint at stronger crystallization induced limitations to chain end mobility during the SwSP at 195 °C as compared to the SSP at 250 °C. This could be related to the solvent induced crystallization in PET, and hence we decided to monitor this by DSC and WAXD.

Fig. 4 shows the DSC thermograms during heating of the dried SwSP product (dotted line, IV ~ 1.4 dL/g) and an SSP product (solid line, IV = 1.42 dL/g, sample from SSP at 250 °C as described in our earlier work [12]). The higher melting temperature $T_m = 260$ °C of the SSP product as compared to $T_m = 251$ °C for the SwSP product corresponds to the annealing of the former during the SSP at the higher temperature (250 °C). The higher heat of melting ($\Delta H_m = 60$ J/g) for the SwSP product as compared to ($\Delta H_m = 51$ J/g) for the SSP product indicates that the extent of crystallization ($x_c = \Delta H_m / \Delta H_c$, where $\Delta H_c = 125.6$ J/g is the crystalline heat of melting of PET [57]) is indeed higher in the SwSP product.

Fig. 5 shows a comparison of the WAXD diffractograms of the above SSP sample and the dried SwSP sample. These spectra have already been corrected for background

scattering, and amorphous spectrum has been subtracted while fitting the peaks by Gaussian components. The peaks are indexed according to the known assignments of the triclinic unit cell dimensions for PET [58–61]. The similar peak positions of the SSP and the SwSP samples indicate that the crystalline forms are identical. Calculations from WAXD spectra showed ($x_c = 0.64$) for the SwSP sample and ($x_c = 0.51$) for the SSP sample. Thus, both the DSC and the WAXD data indicate solvent induced crystallization of PET during SwSP in DPE–BP, and hence its possible role in the progress of post-polymerization.

In Fig. 6, we replot the concentrations of the hydroxyl and the acid end-groups, as functions of IV rise during the SwSP. Also shown in the figure as solid lines is a smooth fit to the corresponding data from in our earlier work [12] for SSP (250 °C). Fig. 6 indicates that the concentration of the hydroxyl end groups in SwSP product is comparable to SSP product at similar IV, but the concentration of the carboxylic acid end groups is higher in the SwSP product as compared to SSP product of the same IV. Since IV is more strongly determined by the higher molecular weight fraction, the higher concentration of the acid end groups in the SwSP products can be due to a possible higher concentration of the acid end group carrying low molecular

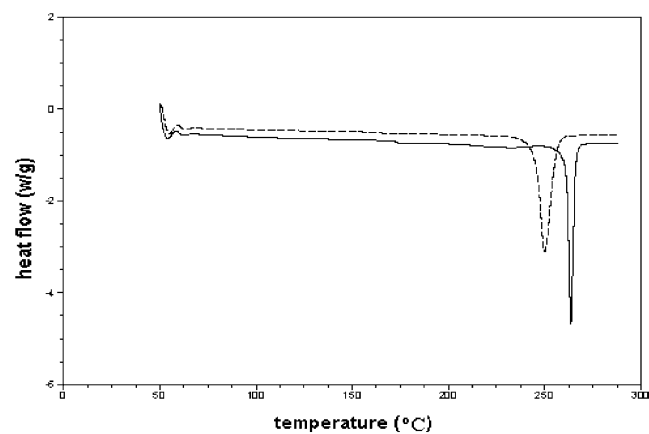


Fig. 4. DSC heating scans of SwSP product (dotted line) and SSP (250 °C, [12]) product (solid line).

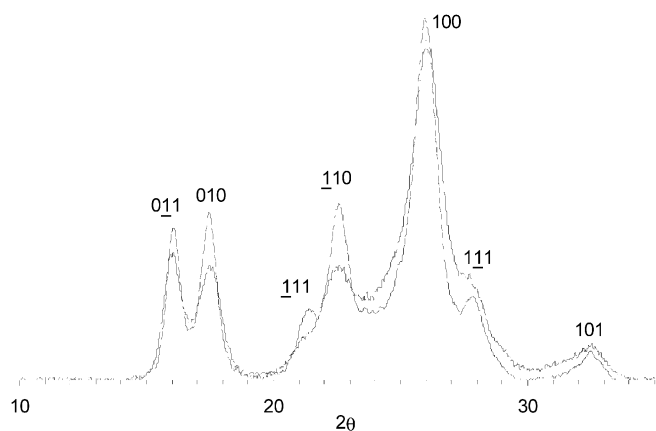


Fig. 5. WAXD scans of SwSP product (solid line) and SSP (250 °C, [12]) product (dotted line).

weight linear polymers. If low molecular weight linear polymers are indeed present in larger amounts in the SwSP product, these would result in its wider molecular weight distribution (MWD) as compared to SSP product of the same IV. We tried to analyze this possibility by comparing SEC (Fig. 7) of PET of IV = 1.37 and 1.40 dL/g obtained by SSP (solid line) and SwSP (dashed line), respectively. As seen from the SEC curves in Fig. 7, we were unable to detect such a tendency, though we note that the SEC resolution was limited to molecular weight higher than about 3000.

3.2. SolP

Since it appears that the extent of SwSP in DPE–BP is limited by the high extent of crystallization, we decided to evaluate if such a limitation can be eliminated by carrying out the post-polymerization by dissolving the PET in the same solvent. Since DPE–BP dissolves PET at about 205 °C, and the boiling points of DPE and BP are 259 and 255 °C, respectively, we carried out the solution polymerization at 250 °C while starting with PET concentration of 30 wt%. Most of the solvent evaporating with the bubbling nitrogen was refluxed by the condenser mounted on the

reactor. However, a small part of the solvent (5% in 30 h), along with the condensates having lower boiling points (EG: $T_b=196$ °C, water: $T_b=100$ °C), was carried over to condense in another water cooled condenser and not returned to the reactor (Fig. 1). Fig. 2 shows the IV vs. time data for post-polymerization of PET of IV = 0.42 dL/g in the solution in DPE–BP at 250 °C. The initial rate of rise of IV during the SolP at 250 °C at 30 wt% concentration is comparable to SwSP at 195 °C at ~56 wt% concentration. It appears that the expected decrease in rate of rise of IV during the lower concentration SolP has been somewhat compensated by the higher temperature as compared to SwSP. However, while the SwSP is hindered beyond IV ~ 1.4 dL/g at ~ 12 h, the SolP continues till IV ~ 1.8 dL/g until ~ 20 h. The lower value of the maximum limiting IV in case of SwSP (with lower amount of solvent as compared to SolP) indicates that this limitation is not dictated by the a chemical influence of the solvent DPE–BP, but perhaps to a physical influence in the solid state, thus possibly through crystallization. In comparison to SolP at 250 °C, the post-polymerization proceeds much faster during an SSP of thin disks (thickness 180 μm) at 250 °C where the IV increases from 0.58 to 2.3 dL/g within 4 h [12]. This can be attributed to the higher concentration and smaller diffusion length during the SSP.

We are aware of only two reported attempts, albeit somewhat unsuccessful, of post-polymerization of PET in solutions. Izard and Auispos [62] found that the solution polymerization of PET in DPE–BP proceeded to IV no higher than 0.72 dL/g. Similarly, Ha et al. [46] found that while solution polymerization of PET of IV = 0.62 dL/g at 220 °C resulted in no IV increase in solvents benzophenone, DPE and terphenyl, the IV increased to 0.87 dL/g in 15 h in the solvent BP. An important advantage of SolP as compared to SwSP and SSP processes for the very high molecular weight PET is the ease of handling a solution polymerization in a standard stirred reactor, as compared to handling of thin films or fine particles while avoiding their fusion during SSP and SwSP at temperatures close to the melting points. Finally, further processing of such high IV

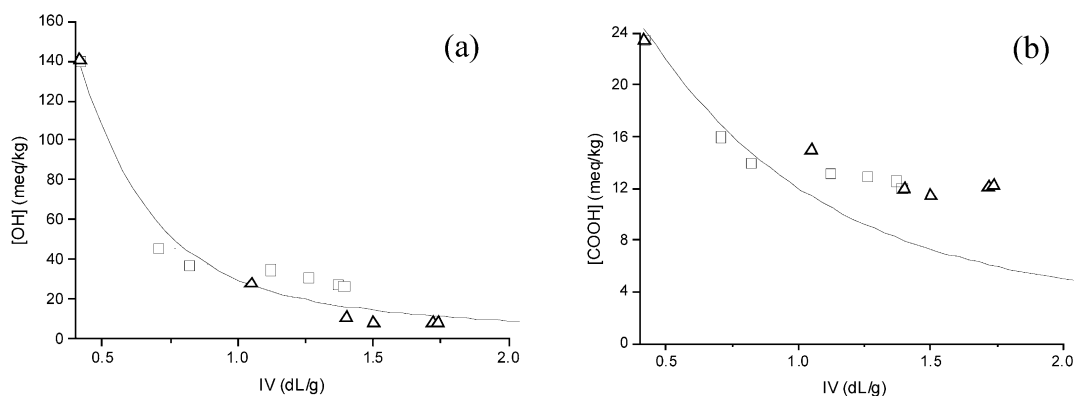


Fig. 6. Depletion of the (a) hydroxyl and (b) acid end-groups with increase in IV during SwSP at 195 °C (squares) and SolP at 250 °C (triangles). The lines represent the SSP (250 °C) data from our previous work [12].

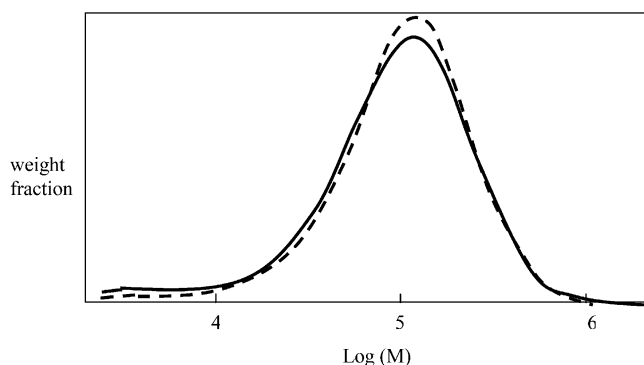


Fig. 7. SEC plots of PET of IV = 1.37 and 1.40 dL/g obtained by SSP (solid line) and SwSP (dashed line), respectively. The respective M_w values are 132,000 and 134,000, and the M_w/M_n values are 2.66 and 2.25. The triple detection SEC measurements were carried out at Akzo Nobel R&T (Arnhem) using PET concentration of about 2 mg/mL in HFIP flowing at 0.6 mL/min.

PET into fibers necessarily demands solubilization in suitable solvents. Since DPE–BP has been found to be a suitable solvent for such processing [50], the use of these solvents during the post-polymerization step poses no disadvantage (such as an additional step to remove solvent at the intermediate stage) as it would allow direct spinning of the solution polymerized high IV PET. While withdrawing the samples from the reactor at the end of the SolP with a stiff wire, we noticed that filaments were drawn out with the wire, thus indicating the sufficient elasticity and the direct spinnability of the SolP product. We found that these filaments (diameter $\sim 200 \mu\text{m}$) could be dried overnight at 150°C under vacuum, and then drawn at 250°C to a draw ratio of seven, resulting in fibers of modulus 11 GPa and strength of 0.47 GPa [63]. We believe that it may be possible to further optimize the process parameters to enhance these properties.

4. Conclusions

We have carried out post-polymerization of PET in presence of the solvent mixture diphenyl ether–biphenyl (DPE–BP). As compared to SSP, the incorporation of solvent during SwSP at 195°C enhances the initial rate of reaction due to the solvent induced mobility, but slows dramatically at $\text{IV} > 1.2 \text{ dL/g}$ due to the restricted mobility of a part of the chain-ends due to crystalline restraints. This is verified by detection of substantial concentration of the hydroxyl and acid end-groups even at the end of SwSP, high extent of crystallization of the SwSP product, and further post-polymerization only after melting to impart mobility to these end-groups. At a higher temperature, PET can be dissolved in the same solvent, permitting post-polymerization in solution. The solution polymerization at 250°C with PET concentration of 30 wt% proceeds from $\text{IV} = 0.42$ to 1.8 dL/g in a single step, and is thus a potentially

attractive route for obtaining solutions of high molecular weight PET, suitable for direct processing into fibers and films.

Acknowledgements

The authors are grateful to M.M.R.M. Hendrix for WAXD, to W.K. Gerritsen for DSC, and to M.S.J.H. Groot for SEC measurements.

References

- [1] Ito M, Takahashi K, Kanamoto T. *J Appl Polym Sci* 1990;40:1257.
- [2] Ziabicki A. *Text Res J* 1996;66:705.
- [3] Huang B, Tucker PA, Cuculo JA. *Polymer* 1997;38:1101.
- [4] Hsu L-C. *J Macromol Sci, Phys* 1967;B1(4):801.
- [5] Cohn G. *Polym Prepr* 1989;30:160.
- [6] Cohn G. US Patent 4792573; 1988.
- [7] Rinehart VR. US Patent 4755587; 1988.
- [8] Ito M, Wakayama Y, Kanamoto T. *Polymer* 1992;48:569.
- [9] Ito M, Wakayama Y, Kanamoto T. *Sen-i Gakkaishi* 1994;35:1210.
- [10] Sasaki I, Hiroshi M, Masaharu F. EP0182352; 1985.
- [11] Boiko YM, Marikhin VA. *Polym Sci USSR Ser A* 2000;42:1169.
- [12] Ma Y, Agarwal US, Sikkema DJ, Lemstra PJ. *Polymer* 2003;44:4085.
- [13] Schaaf E, Zimmerman H, Dietzel W, Lohmann P. *Acta Polym* 1981; 32:250.
- [14] Ravindranath K, Mashelkar RA. *Chem Eng Sci* 1986;41:2197.
- [15] Chen S-A, Chen F-L. *J Polym Sci, Part A: Polym Chem* 1987;25:533.
- [16] Duh B. *J Appl Polym Sci* 2002;83:1288.
- [17] Marechal E. Polyesters: synthesis and chemical aspects. In: Fakirov S, editor. *Handbook of thermoplastic polyesters*, vol. I. New York: Wiley; 2002. p. 1.
- [18] Gantillon B, Spitz R, McKenna TFL. *Macromol Mater Eng* 2004;289: 88.
- [19] Aharoni SM. Industrial scale production of polyesters. In: Fakirov S, editor. *Handbook of thermoplastic polyesters*, vol. I. New York: Wiley; 2002. p. 56.
- [20] Kim TY, Lofgren EA, Jabarin SA. *J Appl Polym Sci* 2003;89:197.
- [21] Chen FC, Griskey RG, Beyer GH. *AIChE J* 1969;15:680.
- [22] Jabarin SA, Lofgren EA. *J Appl Polym Sci* 1986;32:5315.
- [23] Ravindranath K, Mashelkar RA. *J Appl Polym Sci* 1990;39:1325.
- [24] Fakirov S. Solid state reactions in linear polycondensates. In: Schultz JM, Fakirov S, editors. *Solid state behavior of linear polyesters and polyamides*. NJ, USA: Prentice-Hall; 1990. p. 1.
- [25] Devotta I, Mashelkar RA. *Chem Eng Sci* 1993;48:1859.
- [26] Zhi-Lian T, Gao Q, Nan-Xun H, Sironi C. *J Appl Polym Sci* 1995;57: 473.
- [27] Huang B, Walsh JJ. *Polymer* 1998;39:699.
- [28] Duh B. *J Appl Polym Sci* 2001;81:1748.
- [29] Gaymans RJ, Amrithraj J, Kamp H. *J Appl Polym Sci* 1982;27:2513.
- [30] Kaushik A, Gupta SK. *J Appl Polym Sci* 1992;54:507.
- [31] Warner SB, Lee J. *J Polym Sci, Polym Phys Ed* 1994;32:1759.
- [32] Srinivasan R, Almonacil C, Narayan S, Desai P, Abhiraman AS. *Macromolecules* 1998;31:6813.
- [33] Kang C-K. *J Appl Polym Sci* 1998;68:837.
- [34] Mallon FK, Ray WH. *J Appl Polym Sci* 1998;69:1233.
- [35] Wu D, Chen F, Li R, Shi Y. *Macromolecules* 1997;30:6737.
- [36] Boiko YM, Marikhin VA. *Polym Sci USSR Ser A* 2000;42:1169.
- [37] Karayannis GP, Kokkalas DE, Bikiaris DN. *J Appl Polym Sci* 1995; 56:405.
- [38] Gao Q, Nan-Xun H, Zhi-Lian T, Gerking L. *Chem Eng Sci* 1997;52:371.
- [39] Lee EH, Yeo YK, Choi KY, Kim HY. *J Chem Eng Jpn* 2003;36:912.

- [40] Gupta SK, Kumar A. Reaction engineering of step growth polymerization. New York: Plenum; 1987 p. 285.
- [41] Medellin-Rodriguez FJ, Lopez-Guillen R, Waldo-Mendoza MA. J Appl Polym Sci 2000;75:78.
- [42] Tate S, Watanabe Y, Chiba A. Polymer 1993;34:4974.
- [43] Tate S, Ishimaru F. Polymer 1995;36:353.
- [44] Tate S, Watanabe Y. Polymer 1995;36:4991.
- [45] Burke ALV, Marier G, DeSimone JM. Polym Mater Sci Eng 1996;74: 248.
- [46] Ha WS, Oh SK, Youg JH. J Korean Fiber Soc 1990;27:66.
- [47] Wang L-X, Chen F, Wu D-C, Huang L-K, Ma Z-Y, Xiang S-W. J Sichuan Univ (Eng Sci Ed) 2001;33:77.
- [48] Parashar MK, Gupta RP, Jain A, Agarwal US. J Appl Polym Sci 1998; 67:1589–95.
- [49] Tate S, Chiba A, Tani K. Polymer 1996;37:4421.
- [50] Rogers V. EP 0336 556 A2; 1989.
- [51] Ma Y, Agarwal US, Vekemans JAJM, Sikkema DJ. Polymer 2003;44: 4429.
- [52] Solomon OF, Ciuta IZ. J Appl Polym Sci 1962;6:683.
- [53] Koepp HM, Werner H. Makromol Chem 1959;32:79.
- [54] Conix A. Makromol Chem 1958;26:226.
- [55] Griehl W, Neue S. Faserforsch Textiltechn 1954;5:423.
- [56] Kenwright AM, Peace SK, Richards RW, Bunn A, MacDonald WA. Polymer 1998;40:2035.
- [57] Fakirov S, Fischer EW, Hoffman R, Schmidt GF. Polymer 1977;18: 1121.
- [58] Fakirov S, Fischer EW, Schmidt GF. Makromol Chem 1975;176: 2459.
- [59] Bunn CW. In: Hill R, editor. Fibers from synthetic polymers. Amsterdam: Elsevier; 1953 [chapter 11].
- [60] Johnson JE. J Appl Polym Sci 1959;2(5):205.
- [61] Von Kilian HG, Halboth H, Jenckel E. Kolloid-Z 1960;172(2):166.
- [62] Izard EF, Auspos LA, US Patent 2597643; 1952.
- [63] Ma Y, Agarwal US, Yang XN, Zheng X, Loos J, Hendrix MMRM, et al. Submitted for Polymer.